

Performance Enhancement of a Single Pass Solar Air Heater by Adopting Wire Mesh Absorber Layer

Louay A. Rasheed

Department of Electromechanical Engineering, University of Technology

Jamal A.-K. Mohammed

Department of Electromechanical Engineering, University of Technology

Raed A. Jessam

Department of Electromechanical Engineering, University of Technology

<https://doi.org/10.5109/6792883>

出版情報 : Evergreen. 10 (2), pp.880-887, 2023-06. 九州大学グリーンテクノロジー研究教育センター
バージョン :

権利関係 : Creative Commons Attribution-NonCommercial 4.0 International



Performance Enhancement of a Single Pass Solar Air Heater by Adopting Wire Mesh Absorber Layer

Louay A. Rasheed¹, Jamal A.-K. Mohammed¹, Raed A. Jessam^{1,*}

¹Department of Electromechanical Engineering, University of Technology, Baghdad, Iraq

*E-mail: 50097@uotechnology.edu.iq

(Received February 16, 2023; Revised April 12, 2023; accepted April 13, 2023).

Abstract: Solar air heaters are used for air heating, which is subsequently used for greenhouses warming and dry agricultural products. The performance of solar air heaters may be enhanced quite effectively adopting artificial surface geometry. In the current work, an absorber plate design with wire mesh layer in front pass typical solar air heater was examined and compared to a traditional flat absorber plate. Experimental investigation was conducted outside for three values of mass flow rates of 0.05 kg/s, 0.08 kg/s, and 0.11 kg/s. The average thermal efficiency is found to be 42.5%, 57.1% and 68.1% of the typical flat absorber plate, while it was 53.3%, 72.6% and 86.2% of flat absorber plate with wire mesh layer technology with the adopted values of flow rate. The newly proposed technique has much higher thermal efficiency than the traditional one. It encourages more uniform airflow through the absorber, augmentation the surface area and increase the rate of heat transfer, which is resulting in greater surface temperatures in the duct. The experimental study results show that the amount of solar radiation, mass flow rate and the geometry of the absorber surface are the main factors which are affecting on the performance of solar air heaters. The suggested absorber plate design, which features a wire mesh surface, might be utilized as an energy-efficient alternative to solar air warmers.

Keywords: flat plate absorber; mass flow rate; single pass solar air heater; thermal efficiency; wire mesh absorber layer.

1. Introduction

Solar Air Heater (SAH) is a type of heat exchanger that is frequently utilized in low-temperature processes. The main component of SAH which turns solar sunlight into heat is the absorber plate. Because of the thermophysical of air, the coefficient of heat transfer between the absorber plate and moving air is low, this is leading to the fundamental drawback of SAHs are having low thermal efficiency. The use of barriers, baffles, extended, corrugated, and finned surfaces on the absorber surface is a highly efficient way to increase the energy efficiency of SAH. The previous studies have many attempts to enhance the efficiency of SAHs. The generated heat from the SAHs can be utilized by several sectors to dry agricultural goods and as supplementary heaters in houses for example, to save electricity during the cold days. Using solar energy for air heating is significantly cleaner and cheaper than air heating using fossil fuels¹.

Experimental study was conducted on five different types of solar air absorbers by Benli² to determine their energy and exergy content. According to the findings, the absorber's surface form has an impact on both the pressure drop and heat transfer coefficient. Four obstacle forms and three distinct combinations were quantitatively

investigated in SAHs by Kulkarni and Kim³. The obstacle with pentagonal geometry performed the best and showed that the performance of SAH influenced by the design and construction of the barrier. Four different kinds of flat plate SAHs' first and second rules of efficiency were examined by Karsli⁴. The findings of the experiment demonstrated that the performance of SAH is greatly impacted by solar radiation and SAH design. Three different kinds of double-flow SAHs incorporating aluminum cans were experimentally studied to determine their energy efficacy. Ozgen *et al.*⁵ found that the barriers or cans assure good airflow to the absorber plate, produce turbulence, and lessen heater dead zones. Tewari and Dev⁶ were examined the performance of an Integrated Photovoltaic Solar Water Heating System with Absorber Coating on Inner Half of the Tube. The highest hot water temperatures for the months of November and April, respectively. For the month of April 2015, the system's overall effectiveness was determined to range between 27 and 31%. Kim *et al.*⁷, analyzed a plant performance for collector with various areas and storage tank with different volumes. Solar thermal rating, annular solar fraction, capital payback period and annualized life cycle saving were all examined. The study's primary goal was to determine the economic benefits of optimizing a solar hot

water plant that provides water to a flight kitchen at 65°C for an average daily energy requirement. Tewari and Dev⁸⁾ were modified a solar water heating system (MSWHS) of 200L storage tank by adopting two kinds of collectors, flat plate and evacuated tube. The maximum temperature of water was recorded in May to be 85 °C of the storage tank and 89 °C of the collector tubes. Gupta and Kaushik⁹⁾ were investigated the effectiveness of SAHs. According to the researchers, these heaters need to have a high aspect ratio, a duct with short length, and a cold air input temperature. Kabeel *et al.*¹⁰⁾ were examined the thermal efficiency of SAHs with various kinds of absorber plate, flat, finned, and v-corrugated plates. The findings proved that the maximum output temperature of the corrugated type of plate SAH was higher than the finned and flat plates by 5°C and 3.5°C with the same mass flow rate. Four different varieties of SAH, including flat plate, sinusoidal corrugated, sinusoidal-protrusion and protrusion were investigated by Li *et al.*¹¹⁾. The findings revealed that the absorber surface shape has an impact on the heat transfer rate and efficiency of SAH. Jalil *et al.*¹²⁾ tested the performance with high air temperature by performing a series of solar air collectors. The findings demonstrated that it is possible to calculate the number of collectors that must be connected in series to achieve the desired output air temperature. Ribes and multi baffles with V-shaped were tested by Jalil *et al.*¹³⁾. The experimental findings explain that the adopting ribs and baffles with the plate collector enhance the performance by 14% compared to the SAH with flat plate collectors. Torul and Pehlivan¹⁴⁾ looked into the impacts of an absorbing surface selection on a SAH with a conical concentrator's efficiency in a two-pass airflow passage. The findings indicated that packing inserted inside the channel of airflow to improve heat transfer produces increased airflow resistance and significantly raises the necessary pumping power. A novel absorber plate having conical springs was examined by Abuşka and Akgül¹⁵⁾ who compared it to a flat plate. They claimed that under all test conditions, the springs offer considerable thermal efficiency improvements, higher surface area, less dead surface, and significantly less shadowing. Conical ribs have been investigated numerically with the collector of SAH over range of Reynolds numbers (4000 to 160000), by Alam and Kim¹⁶⁾. The best value of thermal efficiency was 69.8%.

By reducing the geometrical characteristics of various roughness, the higher-pressure drop may be increased. The ribs or energy promoters which fixed on the surfaces has a wide application to increase pressure coefficient of air flow by reducing its velocity¹⁷⁻¹⁹⁾. By experimenting with several rib placement structures on the surface, like inline, symmetric, and staggered layouts, the authors also looked at the morphologies of the ribs²⁰⁻²⁴⁾. Investigations were also conducted into the SAH's performance with a conical surface. Utilizing the conical surface area led to greater airflow obstruction, greater turbulence impact, and

a greater coefficient of convective heat transfer²⁵⁾. Experimental research was done on the unglazed double pass air flow SAH, cribriform absorber and wire mesh layer. With a higher mass flow rate of 0.018 kg/s, the highest thermal efficiency of 86% was noted by Mahmood²⁶⁾. Experimental research by Jalil and Ali²⁷⁾ examined the performance of steel wool and stainless-steel mesh as porous media in the bottom surface of a double-pass SAH channel. The experimental results demonstrated that a porous medium increases thermal efficiency compared to a non-porous medium. Singh *et al.*²⁸⁾ were tested the impact of adopting two types, inclined fins and wire mesh on the efficiency of SAH. The results demonstrated that the high rates of heat transmission were accomplished by using first type, inclined fins at an angle of 11°. The best enhancement of investigated SAHs was achieved of 30% and 80% with thermal efficiency and thermohydraulic efficiency, respectively.

This work was adopted an experimental test of an adopted absorber plate using wire mesh. Given the agricultural drying process, a high mass flow rate of 0.11 kg/s was used. The influence of wire mesh absorption qualities on SAH efficiency has not yet been sufficiently researched, despite years of research into various SAH designs to increase thermal efficiency. The goal of this paper is to suggest a more effective absorption panel with higher air velocity and mixing inside the SAH duct by employing a wire mesh absorption panel, to enhance the quantity of energy received, decrease the cost of solar energy, and utilize it sustainably.

2. Research methodology

2.1 Experimental setup

This work examined and experimentally evaluated the thermal performance of a SAH with two absorber models a flat plate and wire mesh layer on a flat plate. Two heaters with the same characteristics were put up as part of the experimental setup for this purpose. The SAH and measuring tools make up the majority of the experimental setup. The tests were conducted in May 2022 in Baghdad, Iraq (33.333° latitude and 44.433° longitude). Iraq is situated in a Northern Hemisphere region that is rather favorable for solar energy availability. It was considered that the heater's slope matched to the magnitude of local latitude. The inclined angle of the SAH was adjusted to 35° south. The experiment tests were conducted in sunny weather at time 8:00 a.m. to 5:00 p.m. The entrance and the exit of the air have the dimensions of (60×700) mm. The penetrated transparent surfaces (glasses) of solar radiation have dimensions of (1500 × 900) mm and a thickness of 4 mm. The heating absorbent plate is constructed of metal and measures (900 × 1500 × 1) mm. Polyurethane foam was employed as insulation for the bottom and side surfaces, and the net area of the absorber is (1500 × 800) mm, made from aluminum sheets and

painted with dark black color. Table 1 lists the key characteristics of the heaters, and Figure 1 depicts the SAH experimental setup.

Table 1: Characteristics of the SAHs

Items	Characteristics
Type of flow	Single-front pass
SAH box	Steel sheet 0.80 mm thickness, 900 mm×1500 mm×150 mm
Insulator	50 mm polyurethane foam
Absorber	From Aluminum, 900x1500x1 mm
Glass	4 mm tempered glass, normally ironed, 90% transmittance
Coated absorber	0.20 - 0.49 Emissivity, 0.88-0.94 Absorptivity
Fan	Cross-flow cooling fan (12V, 4.8W)

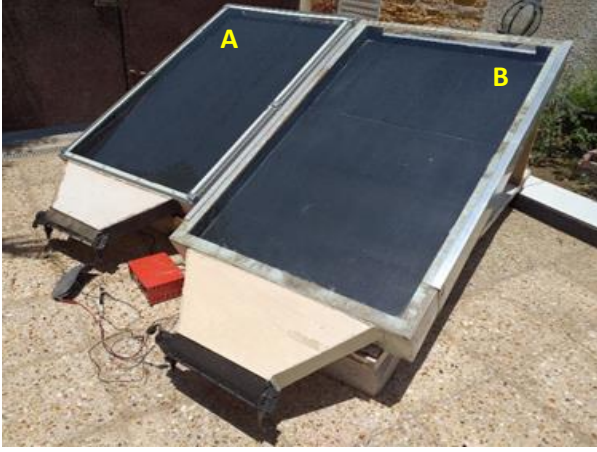


Fig. 1: Experimental setup of two models of SAHs: (A) SAH with wire mesh absorber and (B) SAH with flat plate.

For both investigated SAHs, there is an 8 cm space for moving air between the surface of absorber plate and surface of the glass panel. An aluminum wire mesh with measurements of (1502 × 800) mm has been added to the second SAH. Figure 2 demonstrates the parts of the SAH system with a wire mesh absorber layer. The first part of the SAH system is working on absorbs the solar energy and warms the air by the wire mesh absorber layer. With a 3 degree tilt, the wire mesh is positioned in the duct above the bottom insulation and below the glass cover. The wire mesh layer is fixed on the upper surface of the duct of heater at the inlet of air, while the second end is settled on the lower surface of the duct at the exit of air. The air from the fan enters the duct of the heater and flowing throw the slots of the wire mesh which is installed in an inclined form inside the gap along the duct of SAH. The wire mesh layer has a wire diameter of 0.795 mm and a pitch of 2.5 mm.

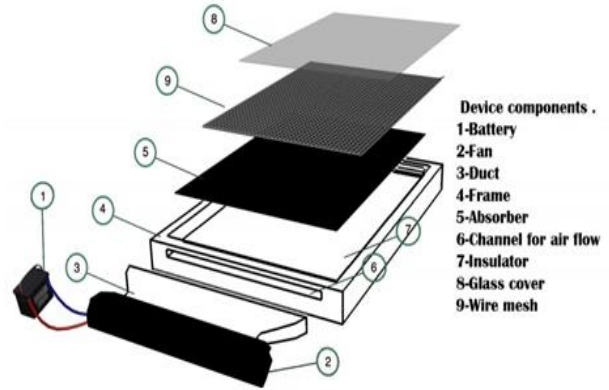


Fig. 2: Components of the SAH combined with wire mesh absorber layer.

2.2 Experimental Procedures

The top view and side view of adopting wire mesh absorber layer of SAH is appear in Figure 3. The basic job of absorber plate is to absorb the heat of the falling solar radiation this process resulting in air heating passes inside the SAH. The advantage of adding wire mesh absorber layer is increasing the temperature of air by reducing the air velocity and increasing thermal conductivity. Three groups of T-type thermocouples were adopted to measuring temperature of T_i , T_o , T_{mesh} and T_p . The T_o temperatures were measured at position 3 cm in front of the orifice meter as shown in Figure 4, were measured by the first group. The wire mesh temperature values T_{mesh} were measured by the second group. While, the plate temperature measurements T_p have been done inside the duct of SAH on the upper surface of absorber plate by the third group. The air was circulated for 30 minutes before the data collection. The time of data collection starts from 8 a.m. to 5 p.m. as well as the relative humidity ratio, wind speed, and solar radiation.

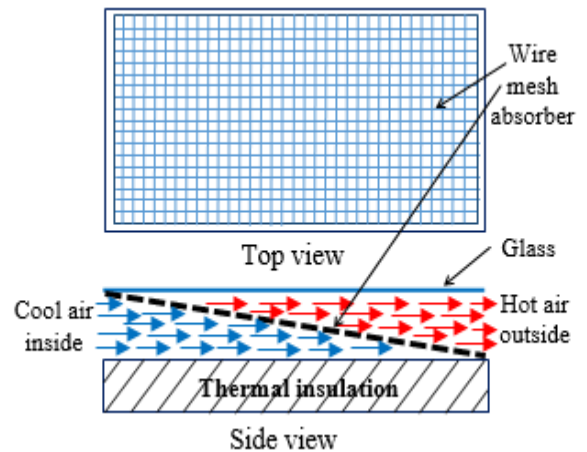


Fig. 3: Schematic assembly of SAH with wire mesh layer absorber.



Fig. 4: The position of measuring the temperature T_o (outlet air) of the SAH.

2.3 Instrumentation

Table 2 lists the experimental measurement instruments together with their accuracy. Three distinct speeds of a cross-flow cooling fan (12 V, 4.8 W, 2200 rpm) were used to provide three different airflow values on a flat plate and wire mesh layer. For the experimental study, three values of mass flow rate values of (0.05, 0.08, and 0.11) kg/s have been achieved. An anemometer was used for the air speed measurement at the exit segment. Measurements were made of the solar radiation intensity (I). Also, the data from a meteorological station situated in the same city was utilized to determine ambient temperatures.

Table 2: Characteristics of the measurement instruments.

Instrument	Accuracy
SM206-SOLAR Solar irradiation meter	$\pm 5\%$ of reading
Lutron (TM-903A), 4 channels temperature data logger	$\pm 0.5\% + 1^\circ\text{C}$
Lutron HT-3007SD Humidity/Temperature Meter	3% reading +1% RH., 0 to 50°C
TES-1341 Hot-Wire Anemometer relative humidity	$\pm 3\%$ RH
UNI-T UT362 anemometer with USB	$(\pm 3\% + 5)$

2.4 Performance parameters

The main thermal performance indicator of SAH is thermal efficiency. Furthermore, several metrics are dependent on air-related characteristics that vary with the of solar radiation intensity, which can be increased or decreased. The average values of the variables that were measured are used in all computations. The equations below are applied to find the indicators to study the performance a SAH.

According to this formula, Q_u , the useful thermal gain is,

$$Q_u = m_a C_p (T_o - T_i) \quad (1)$$

Where:

T_i and T_o : measured temperatures of the inlet and

outlet air, respectively

m_a : air mass flow rate.

C_p : air specific heat.

The mass flow rate of air is given as follows:

$$m_a = \rho A_h V \quad (2)$$

The SAH thermal efficiency can be calculated by the below equation:

$$\eta_{th} = (Q_u / I A_c) \quad (3)$$

The airflow rate in the heater is represented by the Reynolds number:

$$R_e = \frac{V D_h}{\nu} \quad (4)$$

$$D_h = \frac{2WL}{W+L} \quad (5)$$

3. Experimental results

Figure 5 depicts the exterior climatic conditions, solar radiation and temperature, for mass flow rate 0.05 kg/s. It can be noted the peak value of solar radiation in the solar collector inclined plane was measured at 1000 W/m^2 at 13:00 in both cases, with and without using a wire mesh absorber. The surrounding temperature followed a similar pattern to solar radiation and peaked at 13:00.

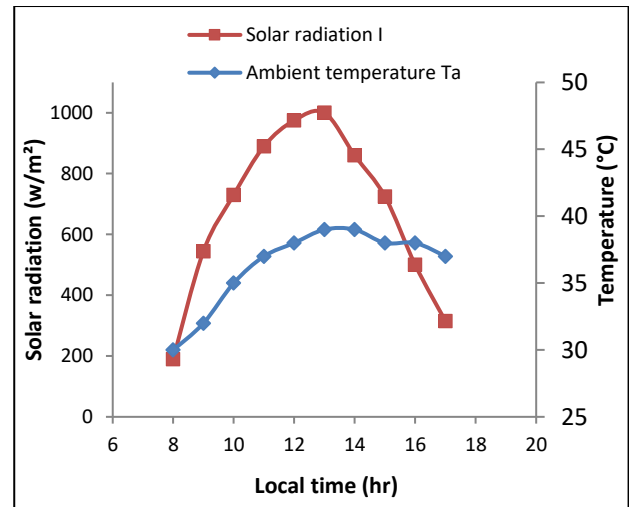


Fig. 5: Change the ambient temperature and solar radiation with standard local time at 0.05 kg/s.

The hourly change in the output air temperature with the two models, absorbent plate surface temperature of the SAH, at a mass flow rate of 0.05 kg/s is shown in Figure 6. The measured temperature of T_{o1} , T_{o2} are ranged between ($31\text{--}50^\circ\text{C}$ and $32\text{--}52^\circ\text{C}$). While it changed between ($33\text{--}73^\circ\text{C}$ and $35\text{--}79^\circ\text{C}$) of T_p and T_{mesh} , respectively. Also, it can observe that the SAH temperature increase with the sun radiation intensity until reaching the peak at 13:00 o'clock. As expected, the output measured temperature of SAH with wire mesh layer is

higher compared to flat plate SAH.

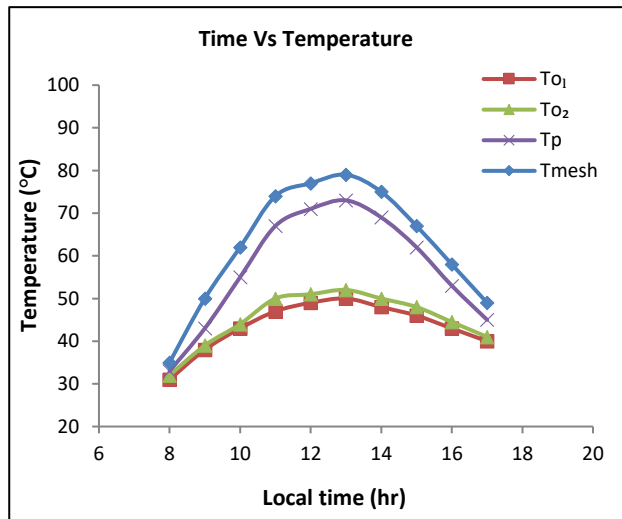


Fig. 6: Measured temperature of the two models and the outlet of SAH with the two models at mass flow rate 0.05 kg/s.

Figure 7 represents the relation between the thermal efficiency of the two models of SAH, with flat plate and with wire mesh layer, during local time at 0.05 kg/s. The higher values of the experimental results of thermal efficiency are 47.1% and 55.74% of SAH with flat and wire mesh layer, respectively. The adopting wire mesh layer absorber increase surface area and create turbulence, which improve the amount of heat transfer by convection between the surface of absorbent plate and air. This process resulting in enhancement the thermal efficiency of SAH by 10.9% with wire mesh layer compared to flat plate.

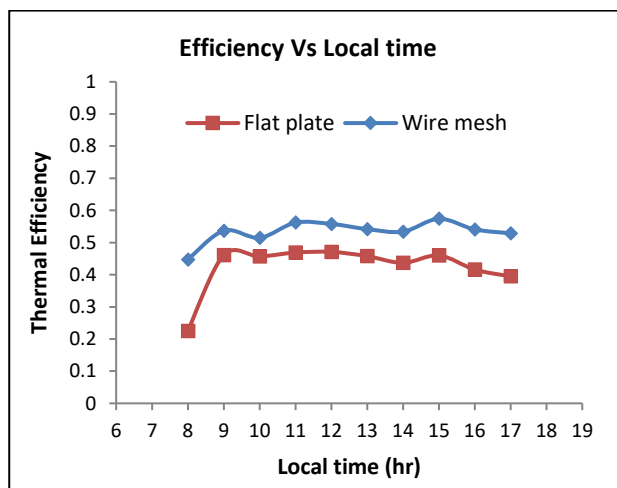


Fig. 7: Variation of thermal efficiency versus local time at 0.05 m/s for SAH flat plate and wire mesh.

The climate conditions, solar radiation and temperature, variation along the local time have been explain in Figure 8. It is observed that the first climate conditions, solar radiation, is increased until reach the maximum value at 998 W/m² around time 13: 00 o'clock and after this time it

starts to decrease. Also, the temperature variation with the local time reaches the maximum value of 39 at 13:00 o'clock, and has similar behavior of change solar radiation.

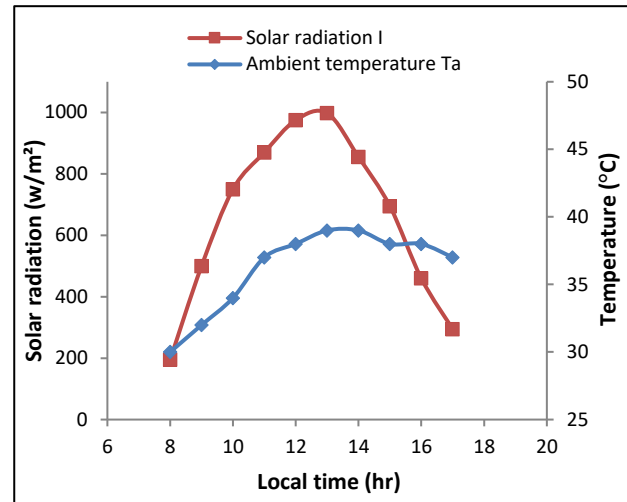


Fig. 8: Change the ambient temperature and solar radiation with standard local time at 0.08 kg/s.

Figure 9 shows the behavior change of measured temperature of wire mesh and flat plate SAH absorbers at 0.08 kg/s. The measured temperature with high and low values were T_{o1} , T_{o2} , T_p and T_{mesh} are 31-48.5°C, 32-50°C, 32-66°C and 36-72°C, respectively. As sun radiation rises in intensity over time, heater temperatures rise as well, reaching their peak around 13:00. The output measured temperature of the SAH with flat plate of is lower than of the SAH with wire mesh surfaces. As a result, the measured temperature at the surface of the flat plate absorber is lower than the measured temperature at the surface of the wire mesh absorber.

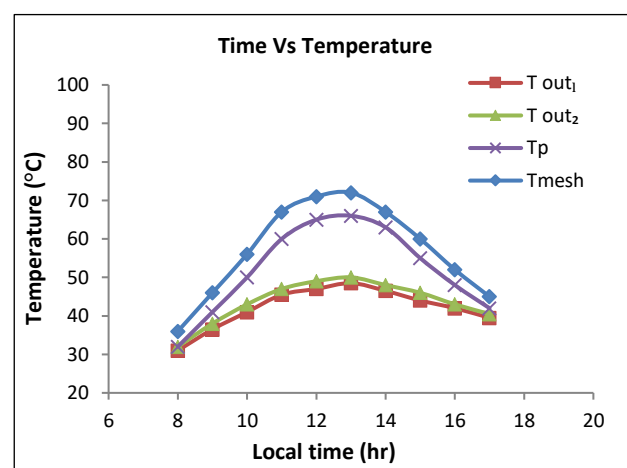


Fig. 9: Measured temperature of the two models and the outlet of SAH with the two models at mass flow rate 0.08 kg/s.

Figure 10 shows the values of the thermal efficiency of the two models of SAH absorbers at a 0.08 kg/s mass flow rate. The experimental values of η_p and η_{mesh} were ranged

between the 44.7-62.7% and 57.6-77% respectively.

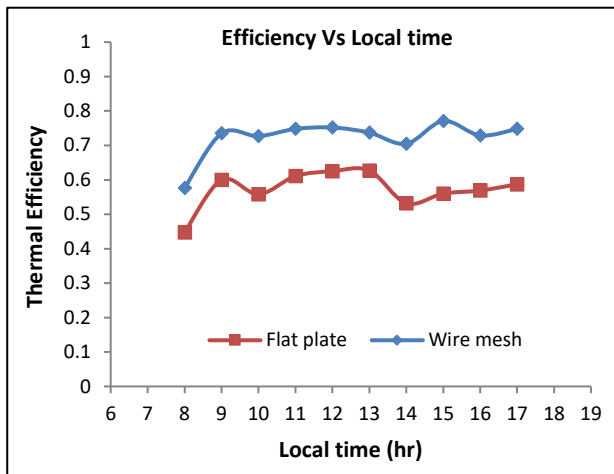


Fig. 10: Variation of thermal efficiency versus local time at 0.08 m/s for SAH flat plate and wire mesh.

The rise in the amount of convection heat transfer rate between the absorber plate and the air result in an improve the thermal efficiency due to the increase surface area and turbulence effect by the wire mesh absorber. Finally, the SAH efficiency was enhanced by 15.5% with applying the wire mesh compared to the SAH without applying the wire mesh.

Figure 11 depicts the exterior climatic conditions for the third day at 0.11 kg/s. It was noticed that the higher measured value of the solar radiation in the solar collector inclined plane was 995 W/m² at 13:00 in both cases. The ambient temperature peaked at 13 o'clock and followed a similar trend to solar radiation.

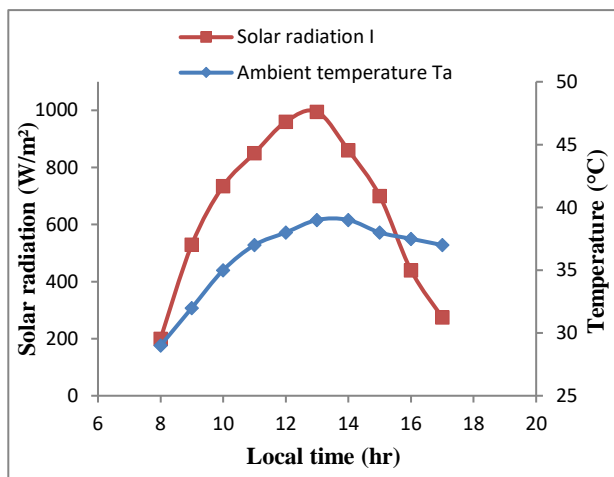


Fig. 11: Change the ambient temperature and solar radiation with local time at 0.11 kg/s.

Figure 12 shows the measured values of temperature of the two absorber models SAH at a mass flow rate of 0.11 kg/s. All the measured values of temperature have similar behavior. The higher values of T_{o1} , T_{o2} , T_p and T_{mesh} are 47°C, 48°C, 61°C and 66°C, respectively. The measured

values of temperature increased as the solar radiation increased until the highest levels around 13:00 o'clock.

As shown in Figure 12, the measured values of temperature at the outlet (T_{out2}) of the SAH with wire mesh surfaces is higher than the outlet temperature of the SAH with flat plate heater (T_{out1}). Also, the temperature of the absorber surface with wire mesh (T_{mesh}) is higher than the temperature of the other absorber type (T_p).

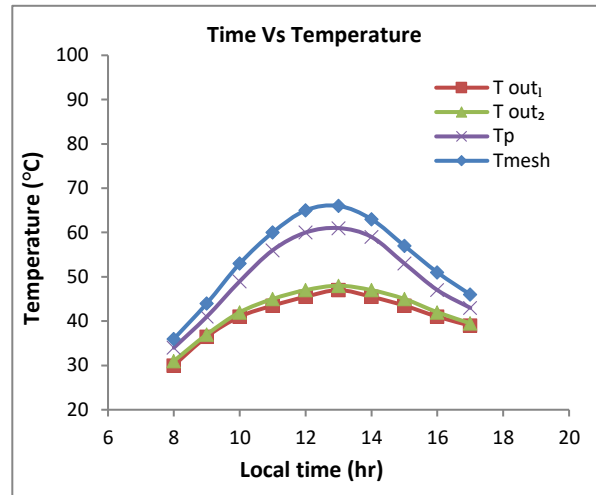


Fig. 12: Measured temperature of the two models and the outlet of SAH with the two models at mass flow rate 0.11 kg/s.

The comparison between the two investigated models, SAH with wire mesh and SAH with flat plate absorbers, with flow velocity of 0.11 kg/s via the thermal efficiency is shows in Figure 13. The observed values of η_p and η_{mesh} were ranged between the minimum and maximum values as (46.1 - 74.3%) and (74.1 - 93.6%), respectively. The wire mesh absorber area allows for increasing in surface area and the turbulence effect, which is leading to improve the amount of heat transfer by convection between the absorbent plate and the surrounding air. This process resulting in increasing the thermal performance of the SAH with wire mesh by 18% compared to SAH without using wire mesh.

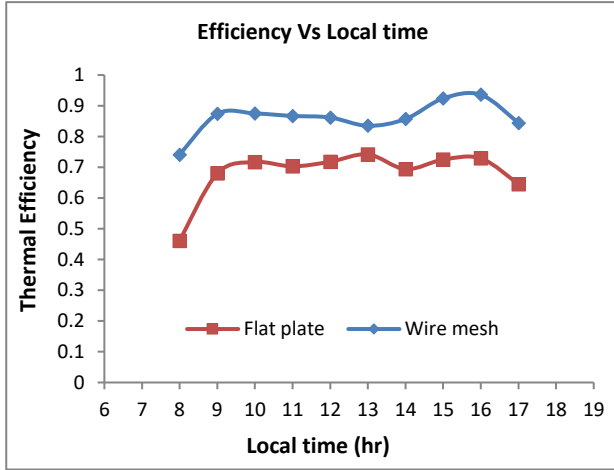


Fig. 13: Variation of thermal efficiency versus local time at 0.11 m/s for SAH flat plate and wire mesh.

Figure 14 explain the thermal effectiveness of the two investigated types of SAH absorbers, with a wire mesh layer and without the wire mesh (flat plate) at different Re numbers. With the different Re, it was noticed that the values of thermal efficiency enhanced with increasing the Re, as predicted. The graphic demonstrates that a wire mesh layer may boost SAH more significantly for each of the three mass flow rate (Reynold numbers). As a result, the SAH with a wire mesh layer operates much more effectively. This is due to the wire mesh layer's increased airflow obstruction, which raises turbulence and the heat transfer coefficient.

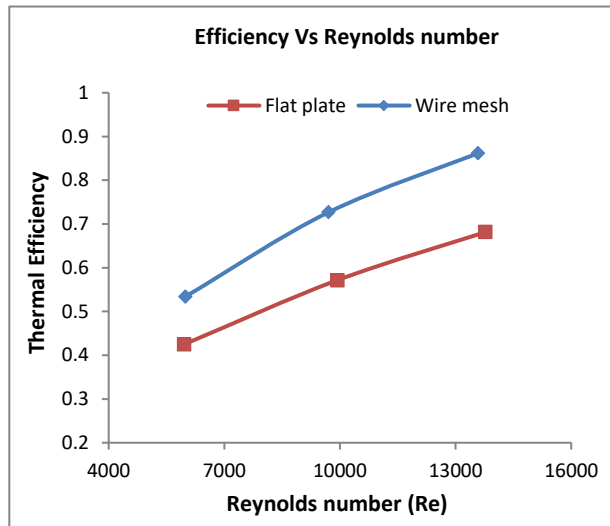


Fig. 14: Thermal efficiency of the two SAH models with range of Reynolds number.

4. Conclusions

In this study the SAH has been investigated experimentally with flat plat absorber and with wire mesh layer absorber at different mass flow rate of air (0.05 kg/s, 0.08 kg/s and 0.11 kg/s). From the collected data and the calculated results, it can be deriving the following

conclusions:

- The thermal efficiency can be enhanced by increase the flow rate and expanding the area of the wire mesh layer. The design of the wire mesh layer absorber improves heat transmission by increasing air vortex generation and air turbulence.
- The enhancement of the absorbed heat by wire mesh layer absorber can be achieved by air flow through wire mesh layers through the gap of the collector. The wire mesh absorption layer absorbs the majority of the solar energy, and by conduction and convection, heat is transferred to the other surfaces of the heater and air.
- Experimental results show that an enhancement of thermal efficiency in employing an expanded wire mesh layer to be 10.9%, 15.5% and 18% against the flat plate model at flow rate 0.05 kg/s, 0.08 kg/s and 0.11 kg/s, respectively.

Acknowledgements

The authors would like to thank the Energy and Renewable Energies Branch / Department of Electromechanical Engineering/ University of Technology for the technical support in conducting this work.

Nomenclature

A_c	Area of collector (m^2)
A_h	Duct cross-section area (m^2)
C_p	Air-specific heat (kJ/kg.K)
D_h	Equivalent hydraulic diameter (m)
I	Global solar radiation (W/m^2)
L	Hight of duct (m)
\dot{m}_a	Air mass flow rate (kg/s)
Q_u	Useful thermal gain (W)
Re	Reynolds number
SAH	Solar air heater
t	Local time (hr)
T_i	Ambient temperature ($^{\circ}C$)
T_{mesh}	Temperature of wire mesh of SAH ($^{\circ}C$)
T_p	Temperature of flat plate of SAH ($^{\circ}C$)
To_1	Temperature of outlet air of flat plate of SAH ($^{\circ}C$)
To_2	Temperature of outlet air of wire mesh of SAH ($^{\circ}C$)
ν	Kinematic Viscosity (m^2/s)
V	Average velocity of air (m/s)
W	Width of duct (m)
η_{th}	Thermal efficiency of the heater (%)
ρ	Air Density (kg/m^3)
ΔT	Temperature difference ($^{\circ}C$)

References

- 1) Akpinar EK, Sarsılmaz C, Yıldız C. Mathematical modeling of a thin layer drying of apricots in a solar energized rotary dryer. *Int J Energy Res.* 28 (2004) 739–52.
- 2) H. Benli, Experimentally derived efficiency and exergy analysis of a new solar air heater having different surface shapes, *Renewable Energy* 50 (2013) 58-67.
- 3) K. Kulkarni, K.Y. Kim, Comparative study of solar air heater performance with various shapes and configurations of obstacles, *Heat and Mass Transfer* 12 (2016) 2795-2811.
- 4) S. Karsli, Performance analysis of new-design solar air collectors for drying applications, *Renewable Energy* 32 (2007) 1645-1660.
- 5) Ozgen,F., M. Esen, H. Esen, Exp. investigation of thermal performance of a double-flow solar air heater having aluminum cans, *Renewable Energy* 34 (2009) 2391-2398
- 6) Dev, R. and Tiwari, G.N. Annual performance of evacuated tubular collector integrated solar still. *Desalination and water Treatment*, 41(1-3), pp.204-223, 2012..
- 7) Kim, Young Deuk, Kyaw Thu, and Kim Choon Ng. "Evaluation and parametric optimization of the thermal performance and cost effectiveness of active-indirect solar hot water plants." *Evergreen* 2, no. 2, 50-60, 2015.
- 8) Tewari, Kirti, and Rahul Dev. "Analysis of modified solar water heating system made of transparent tubes & insulated metal absorber." *Evergreen Joint Journal of Novel Carbon Resource Sciences & Green Asia Strategy* 5, no. 1, 62-72, 2018.
- 9) M.K. Gupta, S.C. Kaushik, Performance evaluation of solar air heater having expanded metal mesh as artificial roughness on absorber plate. *Int. Journal of Thermal Sciences* 48 (2009) 1007- 1016..
- 10) A.E. Kabeel, A. Khalil, S.M. Shalaby, M.E. Zayed, Investigation of the thermal performances of flat, finned, and V-corrugated plate solar air heaters, *ASME Journal of Solar Energy Eng.* 138 (5) (2016).
- 11) S. Li, H. Wang, X. Meng, X. Wei, Comparative study on the performance of a new solar air collector with different surface shapes, *Applied Thermal Engineering* 114 (2017) 639-644.
- 12) J.M. Jalil, K.F. Sultan, and L.A. Rasheed, Numerical and Experimental Investigation of Solar Air Collectors Performance Connected in Series, *Eng. & Tech. Journal* 35A (3) (2018) 798-805.
- 13) J.M. Jalil, G.K. Salih, and Y.A. Madhi, Performance Study of Solar Air Heater with Thermally Conducted Multi V Shaped Baffles and Ribs, *Eng. & Tech. Journal* 36A (8) (2018) 930-938.
- 14) İ.T. Toğrul, D. Pehlivan, Effect of packing in the airflow passage on the performance of a solar air-heater with conical concentrator, *Applied Thermal Engineering* 25 (2005) 1349-1362.
- 15) M. Abuşka, M.B. Akgül, Experimental study on thermal performance of a novel solar air collector having conical springs on absorber plate, *Arabian Journal for Science and Eng.* 41 (2016) 4509-4516.
- 16) T. Alam, M. Kim, Heat transfer enhancement in solar air heater duct with conical protrusion toughness ribs, *Applied Thermal Engineering* 126 (2017) 458-469.
- 17) Jessam, Raed A., Hussain H. Al-Kayiem, and Mohammed S. Nasif. "Flow control in s-shaped air intake diffuser of gas turbine using proposed energy promoters." In *MATEC web of conferences*, vol. 131, p. 02006. EDP Sciences, 2017.
- 18) Jessam, Raed A., Hussain H. Al-Kayiem, and Mohammed Shakir Nasif. "CFD simulation of flow control with energy promoters in S-shaped diffuser." (2017).
- 19) Jessam, Raed A., Hussain H. Al-Kayiem, and Mohammad S. Nasif. "Flow control in s-shaped aggressive diffuser using grooves on the inner and outer surfaces." (2016).
- 20) Singh S,Chander S, Saini JS. Thermo-hydraulic performance due to relative roughness pitch in V-down rib with gap in solar air heater duct - comparison with similar rib roughness geometries. *Renew Sustain Energy Rev.* 43 (2015)1159–66.
- 21) Rajaseenivasan T, Srinivasan S, Srithar K. Comprehensive study on solar air heater with circular and V-type turbulators attached on absorber plate. *Energy* 88 (2015) 863–73.
- 22) Ravi RK, Saini RP. Experimental investigation on performance of a double pass artificial roughened solar air heater duct having roughness elements of the combination of discrete multi V shaped and staggered ribs. *Energy* 116 (2016) 507–16.
- 23) Priyam A, Chand P. Thermal and thermohydraulic performance of wavy finned absorber solar air heater. *Sol Energy* 130 (2016) 250–9.
- 24) Mahmood AJ, Aldabbagh LBY, Egelioglu F. Investigation of single and double pass solar air heater with transverse fins and a package wire mesh layer. *Energy Convers Manag* 89 (2015) 599–607.
- 25) Abus,ka M. Energy and exergy analysis of solar air heater having new design absorber plate with conical surface. *Appl Therm Eng* 131 (2018) 115–24.
- 26) Mahmood AJ. Thermal evaluation of a double-pass unglazed solar air heater with perforated plate and wire mesh layers. *Sustain Times* 12 (2020).
- 27) J.M. Jalil and S.J. Ali, Thermal Investigations of Double Pass Solar Air Heater with Two Types of Porous Media of Different Thermal Conductivity, *Eng. & Tech. Journal* 39A (01) (2021) 79-88.
- 28) Singh S, Dhruw L, Chander S. Experimental investigation of a double pass converging finned wire mesh packed bed solar air heater. *J Energy Storage* 21 (2019) 713–23.